Eur. Phys. J. C 37, 173–184 (2004)
Digital Object Identifier (DOI) 10.1140/epjc/s2004-01979-9

THE EUROPEAN PHYSICAL JOURNAL C

Form factors and semileptonic decay of $D_s^+ \to \phi\bar{\ell}\nu$ from QCD sum rule

Dong-Sheng Du[2,a], Jing-Wu Li[1,b], Mao-Zhi Yang[1,2,c]

[1] CCAST (World Laboratory), P.O. Box 8730, Beijing 100080, China
[2] Institute of High Energy Physics, P.O. Box 918(4), Beijing 100039, China

Received: 14 November 2003 / Revised version: 1 March 2004 /
Published online: 12 August 2004 –

Abstract. We calculate the $D_s^+ \to \phi$ transition form factors V, A_0, A_1 and A_2, and study the semileptonic decay of $D_s^+ \to \phi\bar{\ell}\nu$ based on the QCD sum rule method. We compare our results of the ratios of $V(0)/A_1(0)$, $A_2(0)/A_1(0)$, $\Gamma_{\rm L}/\Gamma_{\rm T}$, and the total decay branching ratio of $D_s^+ \to \phi\bar{\ell}\nu$ with the experimental data and find that they are consistent.

1 Introduction

The semileptonic decay of charm meson is important for studying the strong and weak interactions. It can be used to test techniques developed for solving perturbative and non-perturbative problems in quantum chromodynamics (QCD), and to extract elements of the Cabibbo–Kobayashi–Maskawa (CKM) matrix. Semileptonic decay is simpler than hadronic decay of the charm meson because leptons do not involve the strong interaction. The amplitude of semileptonic decay can be decomposed into several transition form factors due to the Lorentz property of the hadronic matrix element. The form factors include all the non-perturbative effects. Several methods can be used to treat these problems, such as the quark model, the QCD sum rule and lattice QCD, among which the QCD sum rule and lattice QCD are based on first principles of QCD.

The method of QCD sum rules [1] has been widely used in hadronic physics since its establishment in the late 1970s. For semileptonic decays of the charm meson, $D^+ \to \bar{K^0}e^+\nu_e$ was firstly studied by the QCD sum rule method with the three-point correlation function [2]. Several years later, the QCD sum rule method was extended to semileptonic decays of the B meson, $B \to D(D^*)\ell\bar{\nu}$ [3] and $B \to \pi e\nu$ [4]. In these works, the form factors $f_+(q^2)$ and $f_V(q^2)$ are calculated at the point $q^2 = 0$, where q^2 is the momentum transfer squared. For the whole physical region of $0 \le q^2 \le q^2_{\rm max}$, the form factors are either assumed to be under pole dominance, $f(0)/\left(1 - \frac{q^2}{m^2_{\rm pole}}\right)$, or a linear approximation was used. In [5,6], $D \to \bar{K^0}e^+\nu_e$, $\bar{K^0}^*e^+\nu_e$ and $D \to \pi e\nu$, $\rho e\nu$ were studied, where the QCD sum rule method was extended to a very large value of q^2 with a careful treatment of non-Landau-type singularities. D_s decays to the η and η' final states were studied in [7].

In this work, we study $D_s^+ \to \phi\bar{\ell}\nu$ by the QCD sum rule method. This decay mode has been measured in an experiment a long time before [8–11]. Now it is necessary to analyze it theoretically. We perform a calculation up to contributions of operators of dimension 6 in the operator-product expansion (OPE) approach and keep the mass of the s quark. In our result, the large contributions come from the unit operator I (result of perturbative diagram) and a condensate of operators of dimension 3. An operator of dimension 5 gives a smaller contribution. The contributions of operators of dimension 6 are negligible. When calculating the contribution of a perturbative diagram and gluon condensate (operator of dimension 4), Cutkosky's rule has been used. Therefore the subtraction of the continuum contribution is conveniently performed not only for a perturbative diagram but also for the contribution of a gluon condensate. After some long calculation steps, we find that the contributions of the diagrams for the gluon condensate cancel each other, so there is no gluon-condensate contribution in the $D_s^+ \to \phi$ transition. This is our new finding.

There are two independent Borel parameters M_1^2 and M_2^2 in manipulating three-point correlation functions. In general, to simplify the numerical analysis, a fixed ratio of M_1^2/M_2^2 was taken in recent references. In this work, we make the numerical analysis in the whole region of independent M_1^2 and M_2^2 to select the stability "window", so it is different from taking a fixed ratio of these two Borel parameters.

We calculate the $D_s \to \phi$ transition form factors V, A_0, A_1, A_2 and the branching ratio of $D_s^+ \to \phi\bar{\ell}\nu$. Our result of the ratios of $V(0)/A_1(0)$, $A_2(0)/A_1(0)$, $\Gamma_{\rm L}/\Gamma_{\rm T}$ ($\Gamma_{\rm L}$ and $\Gamma_{\rm T}$ denote the decay widths of the D_s^+ to ϕ meson

[a] e-mail: duds@mail.ihep.ac.cn
[b] e-mail: lijw@mail.ihep.ac.cn
[c] e-mail: yangmz@mail.ihep.ac.cn

in longitudinal and transverse polarization, respectively), and the total branching fractions are in agreement with the experimental data.

Recently, just before this work was finished, we found that $D_s^+ \to \phi\bar{\ell}\nu$ was also calculated in [12]. However, this analysis is very different from ours. First, we carefully keep to the requirement that the double Borel parameters M_1^2 and M_2^2 should not be too large for keeping the continuum contribution small, and at the same time, M_1^2 and M_2^2 should not be too small for keeping the truncated OPE series effective, i.e., we keep the contributions of higher dimension operators small, and we get a very different stability "window" for the Borel parameters. Second, our results of the transition form factors are different from theirs. Especially for A_2, these authors got a negative value; however, we get positive one. Using their values of the form factors, although one can get the total branching ratio of $D_s^+ \to \phi\bar{\ell}\nu$ to be compatible with the experimental result, the ratio of $\Gamma_{\rm L}/\Gamma_{\rm T}$ will be too large. But in our case, $\Gamma_{\rm L}/\Gamma_{\rm T} = 0.99 \pm 0.43$, which is consistent with the world average of 0.72 ± 0.18.

This paper is organized as follows. In Sect. 2, we briefly introduce the QCD sum rule method used in this work. Section 3 contains the calculation. Section 4 is the numerical analysis and discussion. Section 5 is devoted to a summary.

2 The method

To calculate the transition form factors of semileptonic D_s meson decays, the standard procedure in the QCD sum rule method is to consider the three-point correlation function defined by

$$\Pi_{\mu\nu} = \mathrm{i}^2 \int \mathrm{d}^4x \mathrm{d}^4y \mathrm{e}^{\mathrm{i}p_2\cdot x - \mathrm{i}p_1\cdot y} \langle 0|T\{j_\nu^\phi(x) j_\mu(0) j_5^D(y)\}|0\rangle, \tag{1}$$

with the currents having the same quantum numbers as the relevant mesonic states under consideration, which are defined by
(1) the current of the D_s channel, $j_5^D(y) = \bar{c}(y)\mathrm{i}\gamma_5 s(y)$;
(2) the current of the weak transition: $j_\mu(0) = \bar{s}\gamma_\mu(1-\gamma_5)c$;
(3) the current of the ϕ channel: $j_\nu^\phi(x) = \bar{s}(x)\gamma_\nu s(x)$.

On one hand, inserting a complete set of intermediate hadronic states into the correlation function, and using the double dispersion relation, one can express the correlation function in terms of a set of hadronic states,

$$\Pi_{\mu\nu} = \int \mathrm{d}s_1 \mathrm{d}s_2 \frac{\rho(s_1, s_2, q^2)}{(s_1 - p_1^2)(s_2 - p_2^2)}, \tag{2}$$

with

$$\rho(s_1, s_2, q^2) = \sum_{XY} \langle 0|j_\nu^\phi|X\rangle\langle X|j_\mu|Y\rangle\langle Y|j_5^D|0\rangle \times \delta(s_1 - m_Y^2)\delta(s_2 - m_X^2)\theta(p_X^0)\theta(p_Y^0),$$

where X and Y denote the complete set of hadronic states of the ϕ and D_s channels, respectively. p_X and p_Y are the four-momentum of the X and Y states, $s_1 = p_Y^2$, $s_2 = p_X^2$, and $q = p_1 - p_2$. Integrating over s_1 and s_2 in (2), we can obtain

$$\Pi_{\mu\nu} = \sum_{XY} \frac{\langle 0|j_\nu^\phi|X\rangle\langle X|j_\mu|Y\rangle\langle Y|j_5^D|0\rangle}{(m_Y^2 - p_1^2)(m_X^2 - p_2^2)} + \text{continuum states}. \tag{3}$$

Separating the ground states of the D_s and ϕ channels, apparently the above equation becomes

$$\Pi_{\mu\nu} = \frac{\langle 0|j_\nu^\phi|\phi\rangle\langle\phi|j_\mu|D_s\rangle\langle D_s|j_5^D|0\rangle}{(m_{D_s}^2 - p_1^2)(m_\phi^2 - p_2^2)} + \text{higher resonances and continuum states}. \tag{4}$$

The weak transition matrix element $D_s \to \phi$ can be decomposed as

$$\begin{aligned}
&\langle\phi(\varepsilon, p_2)|j_\mu|D_s(p_1)\rangle \\
&= \varepsilon_{\mu\nu\alpha\beta}\varepsilon^{*\nu}p_1^\alpha p_2^\beta \frac{2V(q^2)}{m_{D_s} + m_\phi} \\
&\quad -\mathrm{i}\left(\varepsilon_\mu^* - \frac{\varepsilon^*\cdot q}{q^2}q_\mu\right)(m_{D_s} + m_\phi)A_1(q^2) \\
&\quad +\mathrm{i}\left[(p_1 + p_2)_\mu - \frac{m_{D_s}^2 - m_\phi^2}{q^2}q_\mu\right]\varepsilon^*\cdot q\frac{A_2(q^2)}{m_{D_s} + m_\phi} \\
&\quad -\mathrm{i}\frac{2m_\phi\varepsilon^*\cdot q}{q^2}q_\mu A_0(q^2),
\end{aligned} \tag{5}$$

where $q = p_1 - p_2$. The vacuum-to-meson transition amplitudes can be parameterized through defining the corresponding decay constants,

$$\begin{aligned}
\langle 0|\bar{s}\gamma_\nu s|\phi\rangle &= m_\phi f_\phi \varepsilon_\nu^{(\lambda)}, \\
\langle 0|\bar{s}\mathrm{i}\gamma_5 c|D_s\rangle &= \frac{f_{D_s} m_{D_s}^2}{m_c + m_s}.
\end{aligned} \tag{6}$$

Finally the correlation function can be expressed in terms of the meson decay constants and the $D_s \to \phi$ transition matrix element,

$$\Pi_{\mu\nu} = \frac{m_\phi f_\phi \varepsilon_\nu^{(\lambda)}\langle\phi(\varepsilon_\nu^{(\lambda)}, p_2)|j_\mu|D_s(p_1)\rangle f_D m_{D_s}^2}{(m_{D_s}^2 - p_1^2)(m_\phi^2 - p_2^2)(m_c + m_s)} + \text{higher resonances and continuum states}. \tag{7}$$

On the other hand, the correlation function of (1) can be evaluated at negative values of p_1^2 and p_2^2 by the operator-product expansion in QCD, in which the time-ordered current operators in (1) is expanded in terms of a series of local operators with increasing dimensions,

$$\begin{aligned}
&\mathrm{i}^2 \int \mathrm{d}^4x \mathrm{d}^4y \mathrm{e}^{\mathrm{i}p_2\cdot x - \mathrm{i}p_1\cdot y} T\{j_\nu^\phi(x) j_\mu(0) j_5^D(y)\} \\
&= C_{0\mu\nu} I + C_{3\mu\nu}\bar{\Psi}\Psi + C_{4\mu\nu}G_{\alpha\beta}^a G^{a\alpha\beta} \\
&\quad + C_{5\mu\nu}\bar{\Psi}\sigma_{\alpha\beta}T^a G^{a\alpha\beta}\Psi + C_{6\mu\nu}\bar{\Psi}\Gamma\Psi\bar{\Psi}\Gamma'\Psi + \cdots,
\end{aligned} \tag{8}$$

where the $C_{i\mu\nu}$ are Wilson coefficients, I is the unit operator, $\bar{\Psi}\Psi$ is the local fermion field operator of the light

quarks, $G^a_{\alpha\beta}$ is the gluon strength tensor, Γ and Γ' are the matrices appearing in the procedure of calculating the Wilson coefficients. Sandwiching the left- and right-hand sides of (8) between two vacuum states, we get the correlation function in terms of the Wilson coefficients and condensates of local operators,

$$\begin{aligned}\Pi_{\mu\nu} &= \mathrm{i}^2 \int \mathrm{d}^4x \mathrm{d}^4y \mathrm{e}^{\mathrm{i}p_2\cdot x - \mathrm{i}p_1\cdot y}\langle 0|T\{j^\phi_\nu(x) j_\mu(0) j^D_5(y)\}|0\rangle \\ &= C_{0\mu\nu} I + C_{3\mu\nu}\langle 0|\bar{\Psi}\Psi|0\rangle + C_{4\mu\nu}\langle 0|G^a_{\alpha\beta}G^{a\alpha\beta}|0\rangle \\ &+ C_{5\mu\nu}\langle 0|\bar{\Psi}\sigma_{\alpha\beta}T^a G^{a\alpha\beta}\Psi|0\rangle \\ &+ C_{6\mu\nu}\langle 0|\bar{\Psi}\Gamma\Psi\bar{\Psi}\Gamma'\Psi|0\rangle + \cdots \end{aligned} \tag{9}$$

For later convenience, we shall reexpress the above equation. In general, it can be expressed in terms of six independent Lorentz structures

$$\begin{aligned}\Pi_{\mu\nu} &= -f_0 \varepsilon_{\mu\nu\alpha\beta} p_1^\alpha p_2^\beta \\ &- \mathrm{i}(f_1 p_{1\mu} p_{1\nu} + f_2 p_{2\mu} p_{2\nu} + f_3 p_{1\nu} p_{2\mu} \\ &+ f_4 p_{1\mu} p_{2\nu} + f_5 g_{\mu\nu}).\end{aligned} \tag{10}$$

Each f_i includes perturbative and condensate contributions

$$f_i = f_i^{\mathrm{pert}} + f_i^{(3)} + f_i^{(4)} + f_i^{(5)} + f_i^{(6)} + \cdots, \tag{11}$$

where $f_i^{(3)}, \cdots, f_i^{(6)}$ are contributions of condensates of dimension 3, 4, 5, 6, $\cdots$ in (9). In the next section we can see that the perturbative contribution and gluon-condensate contribution can be finally written in the from of this dispersion integration:

$$\begin{aligned} f_i^{\mathrm{pert}} &= \int \mathrm{d}s_1 \mathrm{d}s_2 \frac{\rho_i^{\mathrm{pert}}(s_1, s_2, q^2)}{(s_1 - p_1^2)(s_2 - p_2^2)}, \\ f_i^{(4)} &= \int \mathrm{d}s_1 \mathrm{d}s_2 \frac{\rho_i^{(4)}(s_1, s_2, q^2)}{(s_1 - p_1^2)(s_2 - p_2^2)}. \end{aligned}$$

We approximate the contribution of higher resonances and continuum states as integrations over some thresholds s_1^0 and s_2^0 in the above equations. Then equating the two representations of the correlation function in (7) and (10), we can get an equation for the form factors. To improve such an equation, we make a Borel transformation over p_1^2 and p_2^2 in both sides, which can further suppress higher resonance contributions. The definition of a Borel transformation to any function $f(p^2)$ is

$$\hat{B}\Big|_{p^2,M^2} f(p^2) = \lim_{\substack{n\to\infty \\ p^2\to-\infty \\ -p^2/n = M^2}} \frac{(-p^2)^n}{(n-1)!}\frac{\partial^n}{\partial(p^2)^n} f(p^2).$$

Some examples of the Borel transformation are given in the following:

$$\begin{aligned} &\hat{B}\Big|_{p^2,M^2} \frac{1}{(s-p^2)^k} = \frac{1}{(k-1)!}\frac{1}{(M^2)^k}\mathrm{e}^{-s/M^2}, \\ &\hat{B}\Big|_{p^2,M^2} (p^2)^k = 0, \quad \text{for any} \quad k \geq 0. \end{aligned}$$

Equating the two representations of the correlation function, subtracting the higher resonances and the continuum contribution, and performing the Borel transformation in both variables p_1^2 and p_2^2, we finally obtain the sum rules for the form factors,

$$\begin{aligned} V(q^2) &= \frac{(m_c + m_s)(m_{D_s} + m_\phi)}{2 m_\phi f_\phi f_{D_s} m_{D_s}^2} \\ &\times \mathrm{e}^{m_{D_s}^2/M_1^2}\mathrm{e}^{m_\phi^2/M_2^2} M_1^2 M_2^2 \hat{B} f_0, \\ A_1(q^2) &= -\frac{(m_c + m_s)}{m_\phi f_\phi f_{D_s} m_{D_s}^2 (m_{D_s} + m_\phi)} \\ &\times \mathrm{e}^{m_{D_s}^2/M_1^2}\mathrm{e}^{m_\phi^2/M_2^2} M_1^2 M_2^2 \hat{B} f_5, \\ A_2(q^2) &= \frac{(m_c + m_s)(m_{D_s} + m_\phi)}{m_\phi f_\phi f_{D_s} m_{D_s}^2} \\ &\times \mathrm{e}^{m_{D_s}^2/M_1^2}\mathrm{e}^{m_\phi^2/M_2^2} M_1^2 M_2^2 \frac{1}{2}\hat{B}(f_1 + f_3), \\ A_0(q^2) &= -\frac{(m_c + m_s)}{2 m_\phi^2 f_\phi f_{D_s} m_{D_s}^2}\mathrm{e}^{m_{D_s}^2/M_1^2}\mathrm{e}^{m_\phi^2/M_2^2} M_1^2 M_2^2 \\ &\times \left[\hat{B}(f_1 + f_3)\frac{m_{D_s}^2 - m_\phi^2}{2} + \hat{B}(f_1 - f_3)\frac{q^2}{2} + f_5\right], \end{aligned} \tag{12}$$

where $\hat{B} f_i$ denotes the Borel transformed f_i in both variables p_1^2 and p_2^2, and M_1 and M_2 are Borel parameters. Because we have subtracted the higher resonance and continuum contribution, now the dispersion integration for the perturbative and gluon-condensate contribution should be performed under the threshold,

$$\begin{aligned} f_i^{\mathrm{pert}} &= \int^{s_1^2} \mathrm{d}s_1 \int^{s_2^2} \mathrm{d}s_2 \frac{\rho_i^{\mathrm{pert}}(s_1, s_2, q^2)}{(s_1 - p_1^2)(s_2 - p_2^2)}, \\ f_i^{(4)} &= \int^{s_1^2} \mathrm{d}s_1 \int^{s_2^2} \mathrm{d}s_2 \frac{\rho_i^{(4)}(s_1, s_2, q^2)}{(s_1 - p_1^2)(s_2 - p_2^2)}. \end{aligned}$$

In the next section, we will explain the technique of calculating the Wilson coefficients and give the resulting form of the sum rules for the form factors.

3 The calculation of the Wilson coefficients

In this work, we first calculate the Wilson coefficients in the operator-product expansion [13], then extract the relevant terms f_i for the sum rules of the form factors in (12). We will not present the result of each Wilson coefficient here because their forms are very tedious. We only give the results of the form factors according to the contribution of each condensate.

3.1 The calculation of the perturbative part

The diagram for the perturbative contribution is depicted in Fig. 1. The expansion to leading order in α_s is considered here. This contribution amounts to the Wilson coefficient C_0 in the OPE representation of the correlation function in (9). We can write down this amplitude (see Fig. 1),

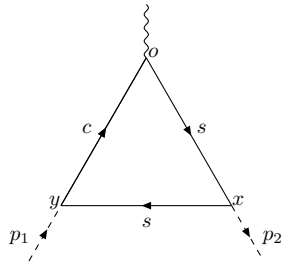

Fig. 1. Diagram for perturbative contribution

$$C_0 = \mathrm{i}^2 \int \frac{\mathrm{d}^4k}{(2\pi)^4}(-1) \times \mathrm{Tr}\left[\mathrm{i}\gamma_5 \frac{\mathrm{i}(\not{k}+m_s)}{k^2-m_s^2+\mathrm{i}\varepsilon}\gamma_\nu \frac{\mathrm{i}(\not{k}+\not{p}_2+m_s)}{(k+p_2)^2-m_s^2+\mathrm{i}\varepsilon} \times\gamma_\mu(1-\gamma_5)\,\frac{\mathrm{i}(\not{k}+\not{p}_1+m_s)}{(k+p_1)^2-m_c^2+\mathrm{i}\varepsilon}\right]. \quad (13)$$

The above integration can be performed according to Cutkosky's rule [14]. That is, we write the integration of (13) in the form of a dispersion integration,

$$C_0 = \int \mathrm{d}s_1\mathrm{d}s_2 \frac{\rho(s_1^2, s_2^2, q^2)}{(s_1-p_1^2)(s_2-p_2^2)}. \quad (14)$$

The spectral density $\rho(s_1, s_2, q^2)$ can be directly calculated by substituting the denominators of the quark propagators for δ functions, i.e., putting all the quark lines on mass shell,

$$\frac{1}{k^2-m_s^2+\mathrm{i}\varepsilon} \to -2\pi\mathrm{i}\delta(k^2-m_s^2), \text{ etc.}; \quad (15)$$

then the spectral density can be calculated from

$$\rho(s_1,s_2,q^2) = \frac{1}{(2\pi\mathrm{i})^2}(-2\pi\mathrm{i})^3 \times \int \frac{\mathrm{d}^4k}{(2\pi)^4}\mathrm{Tr}\left[\gamma_5(\not{k}+m_s)\gamma_\nu(\not{k}+\not{p}_2+m_s)\gamma_\mu(1-\gamma_5) \times(\not{k}+\not{p}_1+m_c)\right]\delta(k^2-m^2)\delta\left[(k+p_1)^2-m_1^2\right] \times\delta\left[(k+p_2)^2-m_2^2\right]\Big|_{\substack{p_1^2\to s_1\\ p_2^2\to s_2}}. \quad (16)$$

To perform the above integration, some basic formulas are needed. Part of them have been given in [15] without the quark mass; here we calculate them with the quark masses included,

$$I = \int \mathrm{d}^4k\delta(k^2-m^2)\delta\left[(k+p_1)^2-m_1^2\right] \times\delta\left[(k+p_2)^2-m_2^2\right] = \frac{\pi}{2\sqrt{\lambda}}, \quad (17)$$

$$I_\mu = \int \mathrm{d}^4k k_\mu\delta(k^2-m^2)\delta\left[(k+p_1)^2-m_1^2\right] \times\delta\left[(k+p_2)^2-m_2^2\right] \equiv a_1p_{1\mu}+b_1p_{2\mu}, \quad (18)$$

$$\begin{cases} a_1 = -\frac{\pi}{2\lambda^{3/2}}[s_2(-s_1+s_2-q^2) \\ \quad +(s_1+s_2-q^2)(m^2-m_2^2) \\ \quad -2s_2(m^2-m_1^2)], \\ b_1 = -\frac{\pi}{2\lambda^{3/2}}[s_1(-s_2+s_1-q^2) \\ \quad +(s_1+s_2-q^2)(m^2-m_1^2) \\ \quad -2s_1(m^2-m_2^2)], \end{cases}$$

$$I_{\mu\nu} = \int d^4k k_\mu k_\nu \delta(k^2-m^2)\delta[(k+p_1)^2-m_1^2]\delta[(k+p_2)^2-m_2^2] \equiv a_2p_{1\mu}p_{1\nu}+b_2p_{2\mu\nu}+c_2(p_{1\mu}p_{2\nu}+p_{1\nu}p_{2\mu})+d_2g_{\mu\nu}, \quad (19)$$

$$\begin{cases} D_1 \equiv s_1-m_1^2+m^2, \quad D_2 \equiv s_2-m_2^2+m^2, \\ a_2 = \frac{\pi}{\lambda^{3/2}}m^2s_2 \\ \quad +\frac{1}{\lambda}[3s_2D_1a_1-(s_1+s_2-q^2)D_2b_1 \\ \quad +s_2D_2b_1], \\ b_2 = \frac{\pi}{\lambda^{3/2}}m^2s_1 \\ \quad +\frac{1}{\lambda}[s_1D_1a_1-(s_1+s_2-q^2)D_1b_1 \\ \quad +3s_1D_2b_1], \\ c_2 = -\frac{\pi}{\lambda^{3/2}}m^2\frac{1}{2}(s_1+s_2-q^2) \\ \quad -\frac{1}{\lambda}\left[\frac{1}{2}(s_1+s_2-q^2)D_1a_1-2s_2D_1b_1 \right. \\ \quad \left. +\frac{3}{2}(s_1+s_2-q^2)D_2b_1\right], \\ d_2 = \frac{\pi}{4\sqrt{\lambda}}+\frac{1}{4}[D_1a_1+D_2b_1], \end{cases}$$

where $\lambda(s_1,s_2,q^2) = (s_1+s_2-q^2)^2-4s_1s_2$, and in (17)–(19) the substitutions $p_1^2 \to s_1$ and $p_2^2 \to s_2$ have been indicated.

3.2 The contribution of the bi-quark operators $\bar{\Psi}(x)\Psi(y)$, $\bar{\Psi}(0)\Psi(x)$

The diagrams for the contributions of $\bar{\Psi}(x)\Psi(y)$ and $\bar{\Psi}(0)\Psi(x)$ are shown in Fig. 2. The contribution of Fig. 2b is zero after a double Borel transformation in both variables p_1^2 and p_2^2 because only one variable appears in the denominator $1/(p_2^2-m_s^2)$. So we will not consider Fig. 2b in the following. The contribution of Fig. 2a to the correlation function is

$$\Pi_{\mu\nu}^{2a} = \mathrm{i}^2\int \mathrm{d}^4x\mathrm{d}^4y\mathrm{e}^{\mathrm{i}p_2\cdot x-\mathrm{i}p_1\cdot y} \times\langle 0|\bar{\Psi}(x)\gamma_\nu\mathrm{i}S_{\mathrm{F}}^s(x)\gamma_\mu(1-\gamma_5)\mathrm{i}S_{\mathrm{F}}^c(-y)\mathrm{i}\gamma_5\Psi(y)|0\rangle, \quad (20)$$

where $\mathrm{i}S_{\mathrm{F}}^s(x)$ and $\mathrm{i}S_{\mathrm{F}}^c(-y)$ are the propagators of s and c quarks, respectively. Moving the quark field operators $\bar{\Psi}(x)$ and $\Psi(y)$ together, we get

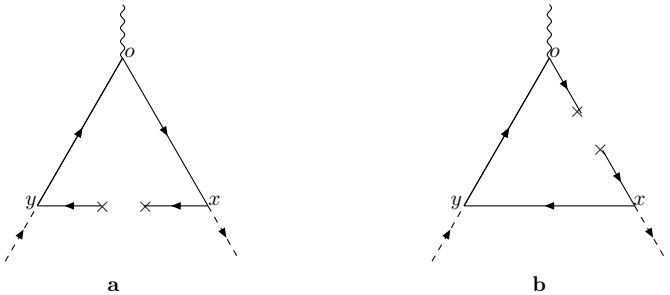

Fig. 2. Diagrams for the contributions of the non-local operators $\bar{\Psi}(x)\Psi(y)$ and $\bar{\Psi}(0)\Psi(x)$

$$\Pi^{2a}_{\mu\nu} = \mathrm{i}^2 \int \mathrm{d}^4x \mathrm{d}^4y \mathrm{e}^{\mathrm{i}p_2\cdot x - \mathrm{i}p_1\cdot y} \times \langle 0|\bar{\Psi}_\alpha(x)\Psi_\beta(y)|0\rangle \left[\gamma_\nu \mathrm{i}S^s_{\mathrm{F}}(x)\gamma_\mu(1-\gamma_5) \times \mathrm{i}S^c_{\mathrm{F}}(-y)\mathrm{i}\gamma_5\right]_{\alpha\beta}, \quad (21)$$

where α and β are Dirac spinor indices. The matrix element $\langle 0|\bar{\Psi}_\beta(x)\Psi_\alpha(y)|0\rangle$ can be dealt with in the fixed-point gauge [16]. We expand it up to the order of x^3 and y^3 using the technique explained in [4,15,17],

$$\begin{aligned}
&\langle 0|\bar{\Psi}^a_\alpha(x)\Psi^b_\beta(y)|0\rangle \\
&= \delta_{ab}\Bigg[\langle\bar{\Psi}\Psi\rangle\left(\frac{1}{12}\delta_{\beta\alpha} + \mathrm{i}\frac{m}{48}(\not{x} - \not{y})_{\beta\alpha}\right. \\
&\left. - \frac{m^2}{96}(x-y)^2\delta_{\beta\alpha} - \frac{\mathrm{i}}{3!}\frac{m^3}{96}(x-y)^2(\not{x} - \not{y})_{\beta\alpha}\right) \\
&+ g\langle\bar{\Psi}TG\sigma\Psi\rangle\left(\frac{1}{192}(x-y)^2\delta_{\beta\alpha}\right. \\
&\left. + \frac{\mathrm{i}}{3!}\frac{m}{192}(x-y)^2(\not{x} - \not{y})_{\beta\alpha}\right) \\
&- \frac{\mathrm{i}}{3!}\frac{g^2}{3^4\times 2^4}\langle\bar{\Psi}\Psi\rangle^2(x-y)^2(\not{x} - \not{y})_{\beta\alpha} + \cdots\Bigg], \quad (22)
\end{aligned}$$

a and b in the above are the color indices, m is the quark mass, and the ellipsis stands for terms of higher orders in the x and y expansion. From (22) we know that Fig. 2a contributes to the coefficients of the quark condensate $\langle\bar{\Psi}\Psi\rangle$, the mixed quark–gluon condensate $g\langle\bar{\Psi}TG\sigma\Psi\rangle$ and the four-quark condensate $\langle\bar{\Psi}\Psi\rangle^2$. Substituting (22) into (21) and integrating over the coordinates x and y, we can explicitly obtain the coefficients of these condensates contributed by Fig. 2a.

3.3 Contributions of the bi-gluon operator $G^a_{\mu\nu}G^{a\mu\nu}$

The diagrams for the contribution of the bi-gluon operator are depicted in Fig. 3. They are calculated in the fixed-point gauge, in which the gauge fixing condition is taken to be $x^\mu A^a_\mu(x) = 0$ [16]. Then the external gauge field can be expressed directly in terms of the color field strength tensor [18]:

$$A^a_\mu(x) = \int_0^1 \mathrm{d}\alpha\alpha x^\rho G^a_{\rho\mu}(\alpha x), \quad (23)$$

which is expanded to the first order to be

$$A^a_\mu(x) = \frac{1}{2}x^\rho G^a_{\rho\mu}(0) + \cdots \quad (24)$$

In the following calculation, it is convenient to transform $A^a_\mu(x)$ to the momentum space,

$$A^a_\mu(k) = -\frac{\mathrm{i}}{2}(2\pi)^2\frac{\partial}{\partial k_\rho}\delta^4(k)G^a_{\rho\mu}(0) + \cdots \quad (25)$$

Then the amplitude can be written down in the momentum space by following the standard Feynman rule.

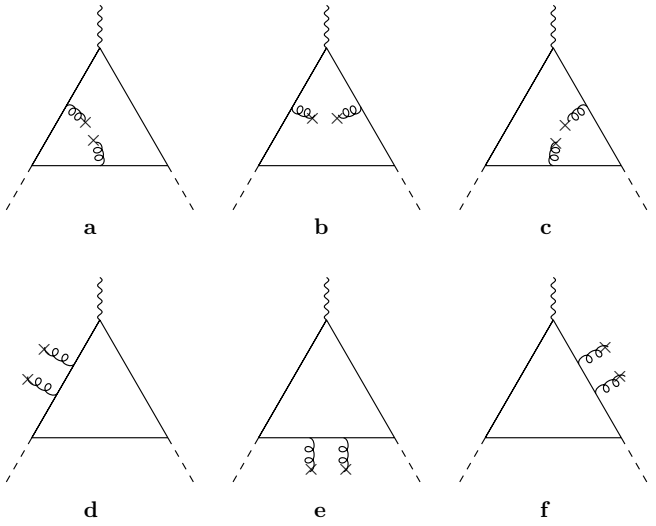

Fig. 3. Diagrams for contributions of the bi-gluon operator

Again, as we did in the previous subsections, we move the gluon strength tensor operator together: $G^a_{\alpha\sigma}G^b_{\beta\rho}$. Then we use the following decomposition to obtain the bi-gluon condensate:

$$\langle 0|G^a_{\alpha\sigma}G^b_{\beta\rho}|0\rangle = \frac{1}{96}\langle GG\rangle\delta_{ab}(g_{\alpha\beta}g_{\sigma\rho} - g_{\alpha\rho}g_{\sigma\beta}), \quad (26)$$

in which $\langle GG\rangle$ is the abbreviation of $\langle 0|G^a_{\mu\nu}G^{a\mu\nu}|0\rangle$.

In the evaluation of the diagrams of Fig. 3 some types of loop integrals encountered are treated first by derivatives with respect to the quark masses, then we transform them to dispersion integrals by using Cutkosky's rule and with the help of the I, I_μ and $I_{\mu\nu}$ functions given previously. For instance,

$$\begin{aligned}
&\int \mathrm{d}^4k \frac{k_\mu k_\nu}{(k^2-m^2)\left[(k+p_2)^2-m_2^2\right]\left[(k+p_1)^2-m_1^2\right]^2} \\
&= \frac{\partial}{\partial m_2^2}\frac{\partial}{\partial m_1^2} \\
&\times \int \mathrm{d}^4k \frac{k_\mu k_\nu}{(k^2-m^2)\left[(k+p_2)^2-m_2^2\right]\left[(k+p_1)^2-m_1^2\right]} \\
&= -2\pi\mathrm{i}\frac{\partial}{\partial m_2^2}\frac{\partial}{\partial m_1^2}\int \mathrm{d}s_1\mathrm{d}s_2\frac{I_{\mu\nu}}{(s_1-p_1^2)(s_2-p_2^2)}, \quad (27)
\end{aligned}$$

and

$$\begin{aligned}
&\int \mathrm{d}^4k \frac{k_\mu k_\nu k\cdot p_2}{(k^2-m^2)^2\left[(k+p_2)^2-m_2^2\right]\left[(k+p_1)^2-m_1^2\right]^2} \\
&= \frac{\partial}{\partial m_2^2}\frac{\partial}{\partial m_1^2} \\
&\times \int \mathrm{d}^4k \frac{k_\mu k_\nu k\cdot p_2}{(k^2-m^2)^2\left[(k+p_2)^2-m_2^2\right]\left[(k+p_1)^2-m_1^2\right]} \\
&= -2\pi\mathrm{i}\frac{\partial}{\partial m^2}\frac{\partial}{\partial m_2^2}\frac{\partial}{\partial m_1^2} \\
&\times \int \mathrm{d}s_1\mathrm{d}s_2\frac{-\frac{1}{2}(s_2-m_2^2+m^2)I_{\mu\nu}}{(s_1-p_1^2)(s_2-p_2^2)}, \quad (28)
\end{aligned}$$

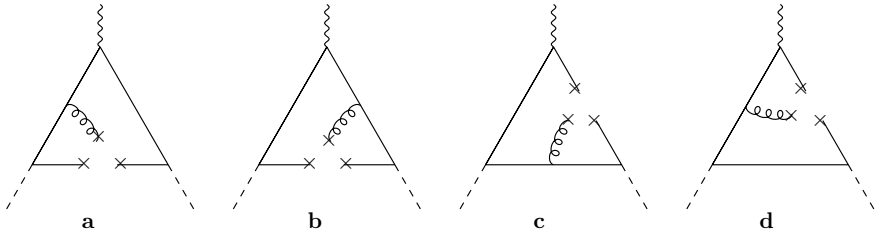

Fig. 4. Diagrams for mixed quark–gluon operators

where the term $-\frac{1}{2}(s_2 - m_2^2 + m^2)$ comes from the δ functions $\delta(k^2 - m^2)\delta\left[(k+p_2)^2 - m_2^2\right]$ with the substitution $p_2^2 \to s_2$ when using Cutkosky's rule.

After some long steps of calculation, we finally find that the contributions of the diagrams (a) to (f) in Fig. 3 cancel each other. Therefore there are no contributions of the gluon condensate in the $D_s \to \Phi$ transition.

3.4 Contributions of quark–gluon mixing and four-quark operators: $\bar{\Psi}(x)\Psi(y)G^a_{\mu\nu}$ and $\langle\bar{\Psi}\Psi\rangle^2$

The diagrams for quark–gluon mixing and four-quark contributions are depicted in Figs. 4 and 5, respectively. The techniques are similar to that explained in the previous subsections. We only give some different points here.

The vacuum average of the non-local quark–gluon mixing operator $\bar{\Psi}(x)\Psi(y)G^a_{\mu\nu}$ is calculated to be

$$\begin{aligned}
&\langle 0|\bar{\Psi}^i_\alpha(x)\Psi^j_\beta(y)G^a_{\mu\nu}|0\rangle \\
&= \frac{1}{192}\langle\bar{\Psi}\sigma TG\Psi\rangle(\sigma_{\mu\nu})_{\beta\alpha}T^a_{ji} \\
&+ \left[-\frac{g}{96\times 9}\langle\bar{\Psi}\Psi\rangle^2(g_{\rho\mu}\gamma_\nu - g_{\rho\nu}\gamma_\mu)(x+y)^\rho\right. \\
&\quad +\mathrm{i}(y-x)^\rho\left(\frac{g}{96\times 9}\langle\bar{\Psi}\Psi\rangle^2\right. \\
&\quad \left.\left. + \frac{m}{96\times 4}\langle\bar{\Psi}\sigma TG\Psi\rangle\right)\varepsilon_{\rho\mu\nu\sigma}\gamma_5\gamma^\sigma\right]_{\beta\alpha}T^a_{ji}, \qquad (29)
\end{aligned}$$

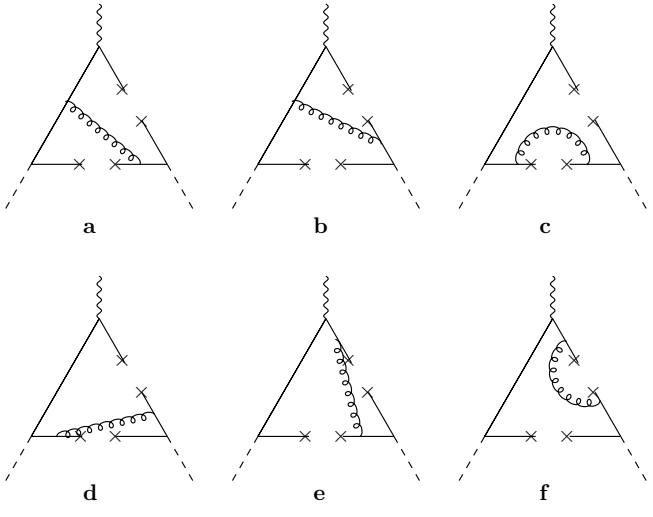

Fig. 5. Diagrams for four-quark contributions

where $\langle\bar{\Psi}\sigma TG\Psi\rangle$ and $\langle\bar{\Psi}\Psi\rangle^2$ are the abbreviations of $\langle 0|\bar{\Psi}\sigma_{\mu\nu}T^aG^{a\mu\nu}\Psi|0\rangle$ and $\langle 0|\bar{\Psi}\Psi|0\rangle^2$, respectively. g is the strong coupling.

Because we calculate up to the condensate of dimension-six operators, the external gluon field $A^a_\mu(x)$ in Fig. 4 should be expanded up to the second term, which will contribute a dimension-six operator,

$$\begin{aligned}
A^a_\mu(x) &= \int_0^1 \mathrm{d}\alpha\alpha x^\rho G^a_{\rho\mu}(\alpha x) \\
&= \frac{1}{2}x^\rho G^a_{\rho\mu}(0) + \frac{1}{3}x^\alpha x^\rho \hat{D}_\alpha G^a_{\rho\mu}(0) + \cdots, \qquad (30)
\end{aligned}$$

where $\hat{D}_\alpha$ is the covariant derivative in the adjoint representation, $(\hat{D}_\alpha)^{mn} = \partial_\alpha\delta^{mn} - gf^{amn}A^a_\alpha$. Then the other vacuum matrix element needed is [15]

$$\begin{aligned}
&\langle 0|\bar{\Psi}^i_\alpha\Psi^j_\beta\hat{D}_\xi G^a_{\sigma\rho}|0\rangle \\
&= -\frac{g}{3^3\times 2^4}\langle\bar{\Psi}\Psi\rangle^2(g_{\xi\rho}\gamma_\sigma - g_{\xi\sigma}\gamma_\rho)_{\beta\alpha}T^a_{ji}\,. \qquad (31)
\end{aligned}$$

We calculate these diagrams and find that the contributions of Figs. 4c,d and 5c,d vanish after double Borel transformation in the two variables p_1^2 and p_2^2, because only one variable is appearing in the denominator; for instance, $\frac{1}{q^2(p_2^2-m_2^2)}$. The Borel transformation in p_1^2 will kill such terms.

Following the above method, after some tedious algebraic derivations with the software MATHEMATICA, we obtain the coefficients f_0, f_1+f_3, f_1-f_3 and f_5 needed in (12). They are listed in the appendix.

4 Numerical analysis and discussion

In the numerical analysis the standard values of the condensates at the renormalization point $\mu = 1\,\mathrm{GeV}$ are taken to be [1,20]

$$\begin{aligned}
\langle\bar{q}q\rangle = -(0.24\pm 0.01\,\mathrm{GeV})^3, \quad \langle\bar{s}s\rangle = m_0^2\langle\bar{q}q\rangle, \\
g\langle\bar{\Psi}\sigma TG\Psi\rangle = m_0^2\langle\bar{\Psi}\Psi\rangle, \quad \alpha_s\langle\bar{\Psi}\Psi\rangle^2 = 6.0\times 10^{-5}\,\mathrm{GeV}^6, \\
m_0^2 = 0.8\pm 0.2\,\mathrm{GeV}^2. \qquad (32)
\end{aligned}$$

The quark masses are fixed to be $m_s = 140\,\mathrm{MeV}$, $m_c = 1.3\,\mathrm{GeV}$ [21], and the decay constant of the ϕ meson is extracted from the experimental data to be $f_\phi = 0.228$ [22]. For the decay constant of the D_s meson we take $f_{D_s} = 0.214\pm 0.038\,\mathrm{GeV}$ [21].

The Borel parameters M_1 and M_2 are not physical parameters. The physical result should not depend on them

Table 1. Requirements to select the Borel parameters M_1^2 and M_2^2 for each form factors $V(0)$, $A_0(0)$, $A_1(0)$ and $A_2(0)$

Form factors	Contribution of condensate	Continuum of D_s channel	Continuum of ϕ channel
$V(0)$	$\leq 49\%$	$\leq 5\%$	$\leq 26\%$
$A_0(0)$	$\leq 29\%$	$\leq 16\%$	$\leq 31\%$
$A_1(0)$	$\leq 49\%$	$\leq 18\%$	$\leq 22\%$
$A_2(0)$	$\leq 11\%$	$\leq 27\%$	$\leq 5\%$

if the operator-product expansion can be calculated up to infinite order. However, OPE has to be truncated to some finite orders in practice. Therefore, the Borel parameters have to be selected in some "windows" to get the best stability of the physical results. The requirement to select the stable "windows" is: the Borel parameters cannot be too large, or contributions of higher resonance and continuum states cannot be effectively suppressed; at the same time, they should not be too small, or the truncated OPE would fail because the series in OPE generally depend on the Borel parameters in the denominator $1/M$. We find the optimal stability with the requirements shown in Table 1 and the thresholds s_1^0, s_2^0 in the ranges $s_1^0 = 5.8$–$6.2\,\mathrm{GeV}^2$, $s_2^0 = 1.9$–$2.1\,\mathrm{GeV}^2$. The regions of the Borel parameters which satisfies the requirements of Table 1 are shown in Fig. 6 in a two-dimensional diagram of M_1^2 and M_2^2. We find good stability of the form factors within these regions.

Because it is not easy to show the contribution of each term of OPE in the two-dimensional regions of M_1^2 and M_2^2, we show the contributions of perturbative and condensate terms in Table 2 at a representative point $(M_1^2,\ M_2^2)$ in the stable region of M_1^2 and M_2^2. In general the higher the dimension of the operators, the smaller the relevant contributions of the condensates. The main contributions to $V(0)$, $A_1(0)$ and $A_2(0)$ are from the perturbative and quark condensate term. For $A_0(0)$, the largest two contributions are from the perturbative term and the mixed quark–gluon condensate. Contributions of the four-quark condensate are less than a few percent; therefore contributions of the operator of dimension 6 are negligible.

The final results for the form factors at $q^2 = 0$ are

$$\begin{aligned} V(0) &= 1.21 \pm 0.33, \\ A_0(0) &= 0.42 \pm 0.12, \\ A_1(0) &= 0.55 \pm 0.15, \\ A_2(0) &= 0.59 \pm 0.17, \\ r_V &\equiv \frac{V(0)}{A_1(0)} = 2.20 \pm 0.85, \\ r_2 &\equiv \frac{A_2(0)}{A_1(0)} = 1.07 \pm 0.43. \end{aligned} \tag{33}$$

We compare our results for the ratios of form factors with the experimental data in Table 3. It shows that the results are consistent with the experimental data.

The physical region for q^2 in $D_s \to \phi\bar{\ell}\nu$ decay extends from 0 to $(m_{D_s} - m_\phi)^2 \simeq 0.9\,\mathrm{GeV}^2$. In the range $q^2 < 0.4\,\mathrm{GeV}^2$, there is no non-Landau-type singularity [5] with the thresholds s_1^0 and s_2^0 chosen in this paper. The q^2 dependence of the form factors is shown in Fig. 7 in the range $-0.4\,\mathrm{GeV}^2 < q^2 < 0.4\,\mathrm{GeV}^2$. Within this range, the behavior of $V(q^2)$ and $A_0(q^2)$ is well compatible with the pole model,

$$V(q^2) = \frac{V(0)}{1 - q^2/m_{\mathrm{pole}}^V},$$

while the q^2 dependence of and $A_1(q^2)$ and $A_2(q^2)$ is very weak.

We fit $V(q^2)$ and $A_0(q^2)$ by the pole model in the range $-0.4\,\mathrm{GeV}^2 < q^2 < 0.4\,\mathrm{GeV}^2$ and extrapolate the fitted result to the whole physical region. The fitted pole masses are

$$\begin{aligned} m_{\mathrm{pole}}^V &= 2.08 \pm 0.13\,\mathrm{GeV}, \\ m_{\mathrm{pole}}^{A_0} &= \ \ 1.9 \pm 0.2\,\mathrm{GeV}. \end{aligned} \tag{34}$$

The form factors calculated by the QCD sum rule in this paper are used to calculate the differential and total decay rate of $D_s \to \phi\bar{\ell}\nu$ decay. There are three polarization states for the ϕ meson: one longitudinal state, two transverse polarization states (right-handed and left-handed). The differential decay rate to the longitudinally polarized ϕ meson is

Table 2. Contributions of perturbative and condensate terms in the operator-product expansion to the form factors $V(0)$, $A_0(0)$, $A_1(0)$ and $A_2(0)$, at a representative point $(M_1^2,\ M_2^2)$ in the stable region of M_1^2 and M_2^2. f^{pert}: perturbative; $f^{(3)}$: quark condensate; $f^{(4)}$: gluon condensate; $f^{(5)}$: mixed quark–gluon condensate; $f^{(6)}$: four-quark condensate

Form factors	total	f^{pert}	$f^{(3)}$	$f^{(4)}$	$f^{(5)}$	$f^{(6)}$	$(M_1^2, M_2^2)\,\mathrm{GeV}^2$
$V(0)$	1.20	0.63	0.66	0	−0.10	0.01	(2.2, 1.4)
$A_0(0)$	0.43	0.28	−0.10	0	0.23	0.02	(1.7, 1.5)
$A_1(0)$	0.53	0.28	0.20	0	0.04	0.01	(2.0, 1.2)
$A_2(0)$	0.57	0.22	0.44	0	−0.09	0.00	(3.6, 1.5)

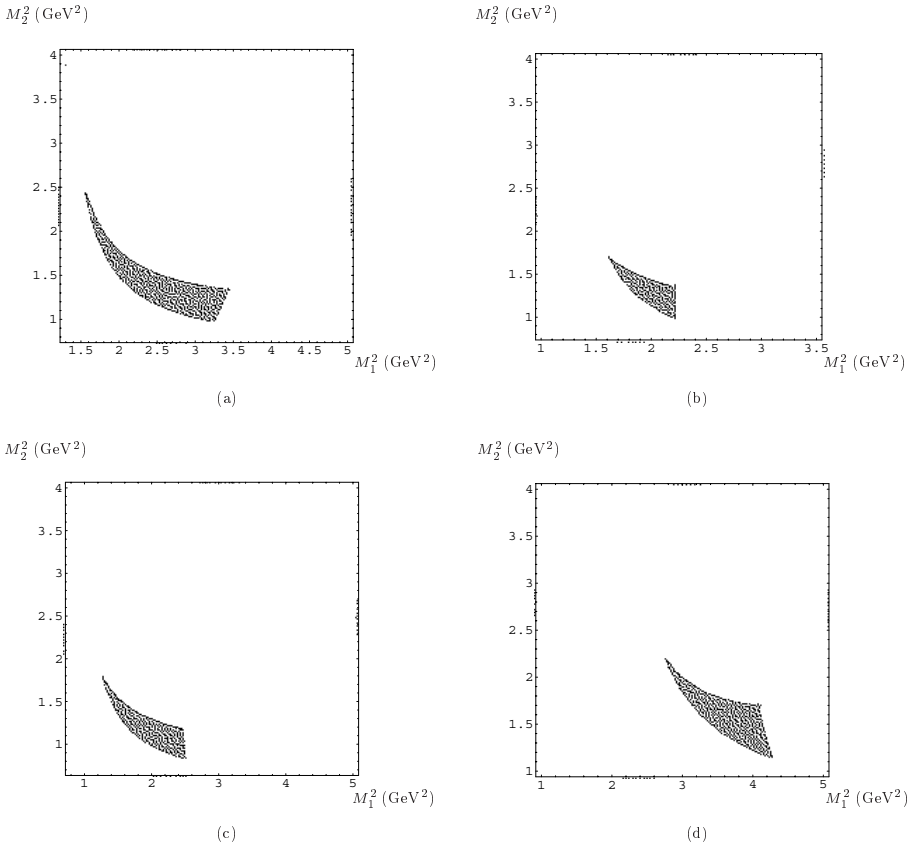

Fig. 6. Selected regions of M_1^2 and M_2^2: **a** for V; **b** for A_0; **c** for A_1; **d** for A_2

$$\frac{\mathrm{d}\Gamma_{\mathrm{L}}}{\mathrm{d}q^2} = \frac{G_{\mathrm{F}}^2|V_{cs}|^2}{192\pi^3 m_{D_s}^3}\sqrt{\lambda(m_{D_s}^2, m_\phi^2, q^2)} \times \left|\frac{1}{2m_\phi}\left[(m_{D_s}^2 - m_\phi^2 - q^2)(m_{D_s}+m_\phi)A_1(q^2) - \frac{\lambda(m_{D_s}^2, m_\phi^2, q^2)}{m_{D_s}+m_\phi}A_2(q^2)\right]\right|^2, \quad (35)$$

where G_{F} is Fermi constant, V_{cs} is CKM matrix element for the $c \to s$ transition, and

$$\lambda(m_{D_s}^2, m_\phi^2, q^2) \equiv (m_{D_s}^2 + m_\phi^2 - q^2)^2 - 4m_{D_s}^2 m_\phi^2.$$

The differential decay rate to the transverse state is

$$\frac{\mathrm{d}\Gamma_{\mathrm{T}}^{\pm}}{\mathrm{d}q^2} = \frac{G_{\mathrm{F}}^2|V_{cs}|^2}{192\pi^3 m_{D_s}^3}\lambda(m_{D_s}^2, m_\phi^2, q^2) \times \left|\frac{V(q^2)}{m_{D_s}+m_\phi} \mp \frac{(m_{D_s}+m_\phi)A_1(q^2)}{\sqrt{\lambda(m_{D_s}^2, m_\phi^2, q^2)}}\right|^2, \quad (36)$$

where the symbols "+" and "−" denote right- and left-handed states, respectively. Finally, the combined transverse and total differential decay rates are

$$\frac{\mathrm{d}\Gamma_{\mathrm{T}}}{\mathrm{d}q^2} = \frac{\mathrm{d}}{\mathrm{d}q^2}(\Gamma_{\mathrm{T}}^+ + \Gamma_{\mathrm{T}}^-), \qquad \frac{\mathrm{d}\Gamma}{\mathrm{d}q^2} = \frac{\mathrm{d}}{\mathrm{d}q^2}(\Gamma_{\mathrm{L}} + \Gamma_{\mathrm{T}}). \quad (37)$$

Table 3. Comparison of our results of r_V and r_2 with experimental data: E791 is from [11], CLEO from [10], E687 from [9] and E653 from [8]

	r_V	r_2
E791	$2.27 \pm 0.35 \pm 0.22$	$1.57 \pm 0.25 \pm 0.19$
CLEO	$0.9 \pm 0.6 \pm 0.3$	$1.4 \pm 0.5 \pm 0.3$
E687	$1.8 \pm 0.9 \pm 0.2$	$1.1 \pm 0.8 \pm 0.1$
E653	$2.3^{+1.1}_{-0.9} \pm 0.4$	$2.1^{+0.6}_{-0.5} \pm 0.2$
average	1.92 ± 0.32	1.60 ± 0.24
our result	2.20 ± 0.85	1.07 ± 0.43

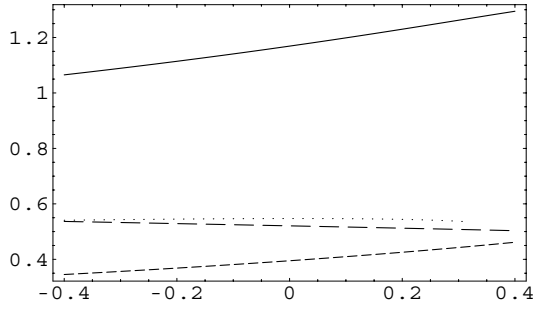

Fig. 7. The q^2 dependence of the form factors from the QCD sum rule. The solid curve is for $V(q^2)$, the short dashed curve for $A_0(q^2)$, the long dashed curve for $A_1(q^2)$, and the dotted one is for $A_2(q^2)$

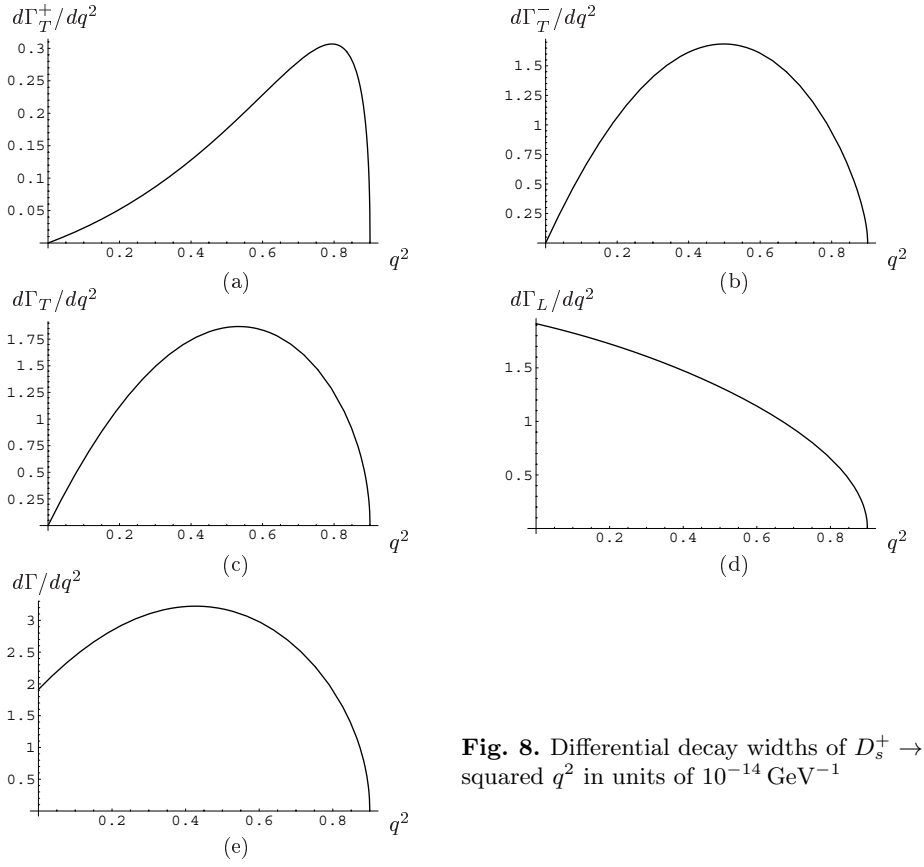

Fig. 8. Differential decay widths of $D_s^+ \to \phi\bar{\ell}\nu$ as a function of momentum transfer squared q^2 in units of $10^{-14}\,\mathrm{GeV}^{-1}$

The differential decay widths as a function of momentum transfer squared q^2 are shown in Fig. 8. We integrate them over q^2 in the whole physical region from $q^2 = 0$ to $(m_{D_s} - m_\phi)^2$ to get the integrated decay widths

$$\begin{aligned} \Gamma_{\mathrm{T}}^+ &= (1.39 \pm 0.75) \times 10^{-15}\,\mathrm{GeV}, \\ \Gamma_{\mathrm{T}}^- &= (1.05 \pm 0.22) \times 10^{-14}\,\mathrm{GeV}, \\ \Gamma_{\mathrm{L}} &= (1.18 \pm 0.43) \times 10^{-14}\,\mathrm{GeV}, \\ \Gamma_{\mathrm{T}} &= (1.19 \pm 0.29) \times 10^{-14}\,\mathrm{GeV}, \end{aligned} \tag{38}$$

and the ratio of $\Gamma_{\mathrm{L}}/\Gamma_{\mathrm{T}}$ is

$$\Gamma_{\mathrm{L}}/\Gamma_{\mathrm{T}} = 0.99 \pm 0.43\,, \tag{39}$$

which is consistent with the averaged experimental data: $(\Gamma_{\mathrm{L}}/\Gamma_{\mathrm{T}})^{\mathrm{exp}} = 0.72 \pm 0.18$ [22]. The detailed comparison of this ratio with experimental data is shown in Table 4.

We use the total decay width of D_s meson $\Gamma_{D_s} = 1.34 \times 10^{-12}$ [22] to obtain the branching ratio of $D_s^+ \to \phi\bar{\ell}\nu$, and our result is

$$\mathrm{Br}(D_s^+ \to \phi\bar{\ell}\nu) = (1.8 \pm 0.5)\%, \tag{40}$$

which is in good agreement with the experimental data: $\mathrm{Br}(D_s^+ \to \phi\bar{\ell}\nu)^{\mathrm{exp}} = (2.0 \pm 0.5)\%$.

Table 4. Comparison of our results of $\Gamma_{\mathrm{L}}/\Gamma_{\mathrm{T}}$ with the experimental data: CLEO from [10], E687 from [9] and E653 from [8]

	$\Gamma_{\mathrm{L}}/\Gamma_{\mathrm{T}}$
CLEO	$1.0 \pm 0.3 \pm 0.2$
E687	$1.0 \pm 0.5 \pm 0.1$
E653	$0.54 \pm 0.21 \pm 0.10$
average	0.72 ± 0.18
our result	0.99 ± 0.43

5 Summary

We calculate the transition form factors for the $D_s \to \phi$ transition in the region $q^2 \leq 0.4\,\mathrm{GeV}^2$ by the QCD sum rule, where no non-Landau-type singularity occurs. Then we fit the result from the QCD sum rule in this region of momentum transfer and extrapolate it to the whole physical region in the decay $D_s^+ \to \phi\bar{\ell}\nu$. We treat the two Borel parameters M_1^2 and M_2^2 as independent parameters and select the allowed region for M_1^2 and M_2^2 by requiring that the higher resonance and continuum contributions in the D_s and ϕ channels are not large, at the same time requiring that the condensate of higher dimension operators do not contribute too much. We find good stability for the transition form factors V, A_0, A_1 and A_2 in the relevant two-dimensional regions of M_1^2 and M_2^2. We obtain the results of the transition form factors V, A_0, A_1 and A_2 in these regions of M_1^2 and M_2^2. Our result of the ratios of these form factors r_V and r_2 are well consistent with the experimental data.

We studied the process $D_s^+ \to \phi\bar{\ell}\nu$ with the form factors calculated by the QCD sum rule. For the transverse polarization state of the final ϕ meson, the rate of D_s decaying to the right-hand state is almost an order smaller than the one for decaying to the left-hand state. The ratio of $\Gamma_{\rm L}/\Gamma_{\rm T}$ and the branching ratio of $D_s^+ \to \phi\bar{\ell}\nu$ are in good agreement with the experimental data within the error bars of both the present experimental data and the theoretical calculation.

Acknowledgements. This work is supported in part by the National Science Foundation of China under contract No.10205017, 90103011, and by the Grant of BEPC National Laboratory.

Appendix

Borel transformed coefficients of perturbative and non-perturbative contributions to the transition form factors in (12) are given here. The contributions of the condensate of the dimension-six operator $\langle\bar{\Psi}\Psi\rangle^2$ are numerically negligible, whereas their expressions are more tedious; therefore we do not present all of them here.
(1) Results for f_0:

$$\hat{B}f_0 = \hat{B}f_0^{\rm pert} + \hat{B}f_0^{(3)} + \hat{B}f_0^{(5)} + \hat{B}f_0^{(6)} \ ,$$

with

$$\begin{aligned}\hat{B}f_0^{\rm pert} &= \int_{4m_s^2}^{s_2^0} {\rm d}s_2 \int_{s_1^{\rm L}}^{s_1^0} {\rm d}s_1 \frac{3{\rm e}^{-s_1/M_1^2 - s_2/M_2^2}}{4M_1^2M_2^2\pi^2\lambda^{3/2}} \\ &\times \left[2s_2m_c^3 - 2s_2m_sm_c^2 - s_2(2m_s^2 + s_1 - s_2 + q^2)m_c \right. \\ &\left. + m_s(-s_2^2 + 2m_s^2s_2 + s_1s_2 + q^2s_2 + \lambda)\right] , \end{aligned} \tag{A1}$$

where $\lambda = (s_1 + s_2 - q^2)^2 - 4s_1s_2$. The lower integration limit $s_1^{\rm L}$ is determined by the condition that all internal quarks are on their mass shell [19],

$$s_1^{\rm L} = \frac{m_c^2}{m_c^2 - q^2}s_2 + m_c^2 \ .$$

We have

$$\begin{aligned}\hat{B}f_0^{(3)} &= -\frac{{\rm e}^{-m_c^2/M_1^2 - m_s^2/M_2^2}}{6M_1^8M_2^8} \\ &\times \left[\left(6M_1^2M_2^6 - 3(M_1^2 + q^2)m_s^2M_2^4 \right.\right. \\ &+ \left.\left.(4(M_1^2 + M_2^2) + q^2)m_s^4M_2^2 - (M_1^2 + M_2^2)m_s^6\right)M_1^4 \right. \\ &+ M_2^2(M_1^2 + M_2^2)m_c^2m_s^2(3M_2^2 - m_s^2)M_1^2 \\ &+ M_2^2m_cm_s(-3M_1^2M_2^4 + (M_1^2 + M_2^2 + q^2)m_s^2M_2^2 \\ &- \left.(M_1^2 + M_2^2)m_s^4)M_1^2 - M_2^4(M_1^2 + M_2^2)m_c^3m_s^3\right] \\ &\times \langle\bar{s}s\rangle \ , \end{aligned} \tag{A2}$$

$$\begin{aligned}\hat{B}f_0^{(5)} &= -\frac{{\rm e}^{-m_c^2/M_1^2 - m_s^2/M_2^2}}{12M_1^8M_2^8} \\ &\times \left[(3M_2^6 - M_1^2M_2^4 + (M_1^2 + M_2^2)m_s^4 \right. \\ &- (3M_2^4 + 5M_1^2M_2^2)m_s^2)M_1^4 \\ &- M_2^2(M_1^2 + M_2^2)m_c^2(3M_2^2 - m_s^2)M_1^2 \\ &+ M_2^2m_cm_s(2M_2^4 - 2M_1^2M_2^2 + (M_1^2 + M_2^2)m_s^2)M_1^2 \\ &+ M_2^4(M_1^2 + M_2^2)m_c^3m_s \\ &+ \left. q^2(M_1^4M_2^2(3M_2^2 - m_s^2) - M_1^2M_2^4m_cm_s)\right] \\ &\times g\langle\bar{s}\sigma TGs\rangle \ , \end{aligned} \tag{A3}$$

$$\begin{aligned}\hat{B}f_0^{(6)} &= \frac{{\rm e}^{-m_c^2/M_1^2 - m_s^2/M_2^2}}{81M_1^8M_2^8(m_c^2 - q^2)m_s^3} \\ &\times \left[18\left(-1 + {\rm e}^{m_s^2/M_2^2}\right)M_1^6(2m_c - m_s)m_sM_2^6 \right. \\ &+ (M_1^2 + M_2^2)m_c^5m_s^3M_2^4 + M_1^2(M_1^2 + M_2^2)m_c^4m_s^4M_2^2 \\ &+ M_1^2q^4m_s^3(m_sM_1^2 + M_2^2m_c)M_2^2 \\ &+ M_1^2m_c^3m_s^3(-13M_2^4 + 2M_1^2M_2^2 + (M_1^2 + M_2^2)m_s^2)M_2^2 \\ &+ M_1^4m_c^2\left(-54\left(-1 + {\rm e}^{m_s^2/M_2^2}\right)M_1^2M_2^6 \right. \\ &+ 54M_1^2m_s^2M_2^4 - (M_1^2 + 10M_2^2)m_s^4M_2^2 + (M_1^2 + M_2^2)m_s^6\big) \\ &+ q^2\left(54\left(-1 + {\rm e}^{m_s^2/M_2^2}\right)M_2^6M_1^6 - 54M_2^4m_s^2M_1^6 \right. \\ &- (M_1^2 + M_2^2)m_s^6M_1^4 - M_2^2(M_1^2 + M_2^2)m_cm_s^5M_1^2 \\ &+ M_2^2(M_1^4 + 10M_2^2M_1^2 - (2M_1^2 + M_2^2)m_c^2)m_s^4M_1^2 \\ &- \left. \left. M_2^2m_c(2M_1^4 - 13M_2^2M_1^2 + (2M_1^2 + M_2^2)m_c^2)m_s^3\right)\right] \\ &\times g^2\langle\bar{s}s\rangle^2 \ . \end{aligned} \tag{A4}$$

(2) Results for $f_1 + f_3$:

$$\hat{B}(f_1 + f_3) = \hat{B}f_+^{\rm pert} + \hat{B}f_+^{(3)} + \hat{B}f_+^{(5)} + \hat{B}f_+^{(6)} \ ,$$

with

$$\begin{aligned}\hat{B}f_+^{\rm pert} &= \int_{4m_s^2}^{s_2^0} {\rm d}s_2 \int_{s_1^{\rm L}}^{s_1^0} \frac{3{\rm e}^{-s_1/M_1^2 - s_2/M_2^2}}{4M_1^2M_2^2\pi^2\lambda^{5/2}} \\ &\times \left\{-6s_2(-s_1 + s_2 + q^2)m_c^5 + 6s_2(-s_1 + s_2 + q^2)m_sm_c^4 \right. \\ &+ 2s_2\left(-4s_1^2 + 8s_2s_1 - 4s_2^2 + 2q^4 - 6(s_1 - s_2)m_s^2 \right. \\ &+ \left.\lambda + 2q^2(3m_s^2 + s_1 + s_2)\right)m_c^3 \\ &+ 2s_2m_s\left[4s_1^2 - 8s_2s_1 + 4s_2^2 - 2q^4 + 6(s_1 - s_2)m_s^2 - 3\lambda \right. \\ &- \left. 2q^2(3m_s^2 + s_1 + s_2)\right]m_c^2 \\ &+ \left[6(s_1 - s_2)s_2m_s^4 \right. \\ &+ 2(4s_2^3 - 8s_1s_2^2 + 4s_1^2s_2 - 2\lambda s_2 + s_1\lambda)m_s^2 \\ &+ (s_1 - s_2)s_2(2s_1^2 - 4s_2s_1 + 2s_2^2 - \lambda) \\ &- 2s_2q^4(2m_s^2 + 2s_1 + s_2) \\ &+ q^2\left(-6s_2m_s^4 - 2(2s_2^2 + 2s_1s_2 + \lambda)m_s^2 \right. \\ &+ \left. \left. s_2(2s_1^2 - 6s_2s_1 + 4s_2^2 - \lambda)\right)\right]m_c \\ &+ m_s\left[2s_2^4 - 6s_1s_2^3 + 6s_1^2s_2^2 - 3\lambda s_2^2 \right. \\ &+ 6(s_2 - s_1)m_s^4s_2 - s_1^3s_2 + 3s_1\lambda s_2 \\ &+ 2q^4(2m_s^2 + 2s_1 + s_2)s_2 + \lambda^2 \\ &- 2(4s_2^3 - 8s_1s_2^2 + 4s_1^2s_2 - 4\lambda s_2 + s_1\lambda)m_s^2 \\ &+ q^2\left(6s_2m_s^4 + 2(2s_2^2 + 2s_1s_2 + \lambda)m_s^2 \right. \\ &+ \left. \left. \left. s_2(-2s_1^2 + 6s_2s_1 - 4s_2^2 + 3\lambda)\right)\right]\right\} \ , \end{aligned} \tag{A5}$$

$$\hat{B}f_+^{(3)} = -\frac{\mathrm{e}^{-m_c^2/M_1^2-m_s^2/M_2^2}}{6M_1^8M_2^8}$$
$$\times \left\{\left[6M_1^2M_2^6 - 3(M_1^2-2M_2^2+q^2)m_s^2M_2^4\right.\right.$$
$$+ \left.(4(M_1^2+M_2^2)+q^2)m_s^4M_2^2 - (M_1^2+M_2^2)m_s^6\right]M_1^4$$
$$+ M_2^2(M_1^2+M_2^2)m_c^2m_s^2(3M_2^2-m_s^2)M_1^2$$
$$- M_2^2m_cm_s(3M_1^2M_2^4 + (M_1^2+M_2^2-q^2)m_s^2M_2^2$$
$$+ \left.(M_1^2+M_2^2)m_s^4)M_1^2 - M_2^4(M_1^2+M_2^2)m_c^3m_s^3\right\}$$
$$\times \langle\bar{s}s\rangle\ , \tag{A6}$$

$$\hat{B}f_+^{(5)} = \frac{\mathrm{e}^{-m_c^2/M_1^2-m_s^2/M_2^2}}{12M_1^8M_2^8}$$
$$\times \left\{\left[(M_1^2+3M_2^2)M_2^4 - (M_1^2+M_2^2)m_s^4\right.\right.$$
$$+ \left.(7M_2^4+5M_1^2M_2^2)m_s^2\right]M_1^4$$
$$+ M_2^2(M_1^2+M_2^2)m_c^2(3M_2^2-m_s^2)M_1^2$$
$$- M_2^2m_cm_s\left[2(M_1^2+2M_2^2)M_2^2 + (M_1^2+M_2^2)m_s^2\right]M_1^2$$
$$- M_2^4(M_1^2+M_2^2)m_c^3m_s$$
$$+ \left.q^2\left[M_2^2(m_s^2-3M_2^2)M_1^4 + M_2^4m_cm_sM_1^2\right]\right\}$$
$$\times g\langle\bar{s}\sigma TGs\rangle\ , \tag{A8}$$

$$\hat{B}f_+^{(6)} = \frac{\mathrm{e}^{-m_c^2/M_1^2-m_s^2/M_2^2}}{81M_1^8M_2^8(m_c^2-q^2)m_s^3}$$
$$\times \left\{-18\left(-1+\mathrm{e}^{m_s^2/M_2^2}\right)M_1^6m_s^2M_2^6\right.$$
$$+ (7M_2^2-2M_1^2)m_c^5m_s^3M_2^4 + M_1^2(M_1^2+M_2^2)m_c^4m_s^4M_2^2$$
$$+ M_1^2q^4m_s^3(M_1^2m_s - 2M_2^2m_c)M_2^2$$
$$+ M_1^2m_c^3m_s^3\left[-26M_2^4 + 4M_1^2M_2^2 + (M_1-2M_2^2)m_s^2\right]M_2^2$$
$$+ M_1^4m_c^2\left[-54\left(-1+\mathrm{e}^{m_s^2/M_2^2}\right)M_1^2M_2^6 + 54M_1^2m_s^2M_2^4\right.$$
$$- 4(M_1^2-2M_2^2)m_s^4M_2^2 + \left.(M_1^2+M_2^2)m_s^6\right]$$
$$+ q^2\left[54\left(-1+\mathrm{e}^{m_s^2/M_2^2}\right)M_1^6M_2^6 - 54M_2^4m_s^2M_1^6\right.$$
$$- (M_1^2+M_2^2)m_s^6M_1^4 - M_2^2(M_1^2-2M_2^2)m_cm_s^5M_1^2$$
$$+ M_2^2(4(M_1^4-2M_1^2M_2^2) - (2M_1^2+M_2^2)m_c^2)m_s^4M_1^2$$
$$+ \left.M_2^4m_c(-4M_1^4 + 26M_2^2M_1^2 + (4M_1^2-7M_2^2)m_c^2)m_s^3\right]\right\}$$
$$\times g^2\langle\bar{s}s\rangle^2\ . \tag{A9}$$

(3) Results for $f_1 - f_3$:

$$\hat{B}(f_1-f_3) = \hat{B}f_-^{\mathrm{pert}} + \hat{B}f_-^{(3)} + \hat{B}f_-^{(5)} + \hat{B}f_-^{(6)}\ ,$$

with

$$\hat{B}f_-^{\mathrm{pert}} = \int_{4m_s^2}^{s_2^0}\mathrm{d}s_2\int_{s_1^{\mathrm{L}}}^{s_1^0}\frac{-3\mathrm{e}^{-s_1/M_1^2-s_2/M_2^2}}{4M_1^2M_2^2\pi^2\lambda^{5/2}}$$
$$\times \left\{6s_2(s_1+3s_2-q^2)m_c^5 - 6s_2(s_1+3s_2-q^2)m_sm_c^4\right.$$
$$+ 2s_2\left[-4s_1^2 - 4s_2s_1 + 8s_2^2 + 2q^4 - 6(s_1+3s_2)m_s^2 + \lambda\right.$$
$$+ \left.2q^2(3m_s^2+s_1-5s_2)\right]m_c^3$$
$$+ 2s_2m_s\left[4s_1^2 + 4s_2s_1 - 8s_2^2 - 2q^4 + 6(s_1+3s_2)m_s^2 + \lambda\right.$$
$$- \left.2q^2(3m_s^2+s_1-5s_2)\right]m_c^2$$
$$+ \left[6s_2(s_1+3s_2)m_s^4\right.$$
$$+ 2(s_1+2s_2)(-4s_2^2+4s_1s_2+\lambda)m_s^2$$
$$+ (s_1-s_2)s_2(2s_1^2-2s_2^2-\lambda)$$
$$+ 2s_2q^4(-2m_s^2-2s_1+s_2)$$
$$+ q^2\left(-6s_2m_s^4 - 2(-10s_2^2+2s_1s_2+\lambda)m_s^2\right.$$
$$- \left.\left.s_2(-2s_1^2-10s_2s_1+4s_2^2+\lambda)\right)\right]m_c$$
$$- m_s\left[2s_2^4 - 2s_1s_2^3 - 2s_1^2s_2^2 - \lambda s_2^2 + 6(s_1+3s_2)m_s^4s_2\right.$$
$$+ 2s_1^3s_2 + s_1\lambda s_2 + 2q^4(-2m_s^2-2s_1+s_2)s_2 - \lambda^2$$
$$+ 2(-8s_2^3 + 4s_1s_2^2 + 4s_1^2s_2 + 4\lambda s_2 + s_1\lambda)m_s^2$$
$$+ q^2\left(-6s_2m_s^4 - 2(-10s_2^2+2s_1s_2+\lambda)m_s^2\right.$$
$$+ \left.\left.\left.s_2(2s_1^2+10s_2s_1-4s_2^2+\lambda)\right)\right]\right\}\ , \tag{A10}$$

$$\hat{B}f_-^{(3)} = \frac{\mathrm{e}^{-m_c^2/M_1^2-m_s^2/M_2^2}}{6M_1^8M_2^8}$$
$$\times \left\{\left[6M_1^2M_2^6 - 3(M_1^2+2M_2^2+q^2)m_s^2M_2^4\right.\right.$$
$$+ \left(4(M_1^2+M_2^2)+q^2\right)m_s^4M_2^2 - (M_1^2+M_2^2)m_s^6\left.\right]M_1^4$$
$$+ M_2^2(M_1^2+M_2^2)m_c^2m_s^2(3M_2^2-m_s^2)M_1^2$$
$$- M_2^2m_cm_s(3M_1^2M_2^4 + (M_1^2-3M_2^2-q^2)m_s^2M_2^2$$
$$+ \left.(M_1^2+M_2^2)m_s^4)M_1^2 - M_2^4(M_1^2+M_2^2)m_c^3m_s^3\right\} \times \langle\bar{s}s\rangle\ , \tag{A11}$$

$$\hat{B}f_-^{(5)} = -\frac{\mathrm{e}^{-m_c^2/M_1^2-m_s^2/M_2^2}}{12M_1^8M_2^8}$$
$$\times \left\{\left[(M_1^2-9M_2^2)M_2^4 - (M_1^2+M_2^2)m_s^4\right.\right.$$
$$+ \left.(5M_1^2M_2^2 - M_2^4)m_s^2\right]M_1^4$$
$$+ M_2^2(M_1^2+M_2^2)m_c^2(3M_2^2-m_s^2)M_1^2$$
$$- M_2^4(M_1^2+M_2^2)m_c^3m_s$$
$$- m_c\left[2M_1^4m_sM_2^4 + M_1^2(M_1^2+M_2^2)m_s^3M_2^2\right]$$
$$+ \left.q^2\left[M_2^2(m_s^2-3M_2^2)M_1^4 + M_2^4m_cm_sM_1^2\right]\right\}$$
$$\times g\langle\bar{s}\sigma TGs\rangle\ , \tag{A13}$$

$$\hat{B}f_-^{(6)} = -\frac{\mathrm{e}^{-m_c^2/M_1^2-m_s^2/M_2^2}}{81M_1^8M_2^8(m_c^2-q^2)m_s^3}$$
$$\times \left\{54\left(-1+\mathrm{e}^{m_s^2/M_2^2}\right)M_1^6m_s^2M_2^6\right.$$
$$+ (7M_2^2-2M_1^2)m_c^5m_s^3M_2^4 + M_1^2(M_1^2+M_2^2)m_c^4m_s^4M_2^2$$
$$+ M_1^2q^4m_s^3(M_1^2m_s - 2M_2^2m_c)M_2^2$$
$$+ M_1^2m_c^3m_s^3\left[-18M_2^4 + 4M_1^2M_2^2 + (M_1-2M_2^2)m_s^2\right]M_2^2$$
$$+ M_1^4m_c^2\left[-54\left(-1+\mathrm{e}^{m_s^2/M_2^2}\right)M_1^2M_2^6 + 54M_1^2m_s^2M_2^4\right.$$
$$- 4(M_1^2+4M_2^2)m_s^4M_2^2 + \left.(M_1^2+M_2^2)m_s^6\right]$$
$$+ q^2\left[54\left(-1+\mathrm{e}^{m_s^2/M_2^2}\right)M_1^6M_2^6\right.$$
$$- 54M_2^4m_s^2M_1^6 - (M_1^2+M_2^2)m_s^6M_1^4$$
$$- M_2^2(M_1^2-2M_2^2)m_cm_s^5M_1^2$$
$$+ M_2^2(4M_1^2(M_1^2+4M_2^2) - (2M_1^2+M_2^2)m_c^2)m_s^4M_1^2$$
$$+ \left.M_2^4m_c(-4M_1^4 + 18M_2^2M_1^2 + (4M_1^2-7M_2^2)m_c^2)m_s^3\right]\right\}$$
$$\times g^2\langle\bar{s}s\rangle^2\ . \tag{A14}$$

(4) Results for f_5:

$$\hat{B}(f_5) = \hat{B}f_5^{\rm pert} + \hat{B}f_5^{(3)} + \hat{B}f_5^{(5)} + \hat{B}f_5^{(6)} \ ,$$

with

$$\begin{aligned}
\hat{B}f_5^{\rm pert} &= \int_{4m_s^2}^{s_2^0} {\rm d}s_2 \int_{s_1^{\rm L}}^{s_1^0} \frac{-3{\rm e}^{-s_1/M_1^2 - s_2/M_2^2}}{8M_1^2M_2^2\pi^2\lambda^{3/2}} \\
&\times \big\{2s_2m_c^5 - 2s_2m_sm_c^4 - 2s_2(2m_s^2 + s_1 - s_2 + q^2)m_c^3 \\
&+ 2s_2m_s(2M - s^2 + s_1 - s_2 + q^2)m_c^2 \\
&+ \big[2s_2m_s^4 + 2(-s_2^2 + s_1s_2 + \lambda)m_s^2 + s_2\lambda \\
&+ 2s_2q^2(m_s^2 + s_1)\big]m_c \\
&- m_s\big[2s_2m_s^4 + 2(-s_2^2 + s_1s_2 + \lambda)m_s^2 - s_1\lambda \\
&+ q^2(2s_2m_s^2 + 2s_1s_2 + \lambda)\big]\big\} \ , \qquad \text{(A15)} \\
\hat{B}f_5^{(3)} &= -\frac{{\rm e}^{-m_c^2/M_1^2 - m_s^2/M_2^2}}{12M_1^8M_2^8} \\
&\times \big\{M_2^4(M_1^2 + M_2^2)m_s^3m_c^5 \\
&- M_2^2(M_1^2 + M_2^2)m_s\big[3M_1^2M_2 - (M_1^2 + 2M_2^2)m_s^2\big]m_c^4 \\
&+ \big[3M_1^4m_sM_2^6 - 9M_1^2(M_1^2 + M_2^2)m_s^3M_2^4 \\
&+ (M_2^6 + 4M_1^2M_2^4 + 3M_1^4M_2^2)m_s^5\big]m_c^3 \\
&+ M_1^2\big[-6M_1^4M_2^6 + (M_1^4 + 4M_2^2M_1^2 + 3M_2^4)m_s^6 \\
&- (6M_2^6 + 11M_1^2M_2^4 + 5M_1^4M_2^2)m_s^4 \\
&+ 3(3M_1^2M_2^6 + 2M_1^4M_2^4)m_s^2\big]m_c^2 \\
&+ M_1^2m_s\big[-15M_1^4M_2^6 + (2M_1^4 + 3M_2^2M_1^2 + M_2^4)m_s^6 \\
&- (2M_2^6 + 13M_1^2M_2^4 + 11M_1^4M_2^2)m_s^4 \\
&+ (8M_1^2M_2^6 + 11M_1^4M_2^4)m_s^2\big]m_c \\
&+ M_1^4m_s^2\big[3M_1^2M_2^6 - 4(M_1^2 + M_2^2)m_s^4M_2^2 \\
&+ (M_1^2 + M_2^2)m_s^6 + (2M_2^6 + 5M_1^2M_2^4)m_s^2\big] \\
&+ M_1^2M_2^2q^4m_s^2\big[(m_s^2 - 3M_2^2)M_1^2 + M_2^2m_cm_s\big] \\
&+ q^2\big[(6M_1^2M_2^6 - (M_1^2 + 2M_2^2)m_s^6 \\
&+ (7M_2^4 + 5M_1^2M_2^2)m_s^4 - 3(M_2^6 + 2M_1^2M_2^4)m_s^2)M_1^4 \\
&+ M_2^2m_c^2m_s^2(3M_2^2(2M_1^2 + M_2^2) - (2M_1^2 + 3M_2^2)m_s^2)M_1^2 \\
&+ M_2^2m_cm_s(-3M_1^2M_2^4 - (3M_1^2 + 2M_2^2)m_s^4 \\
&+ (2M_2^4 + 9M_1^2M_2^2)m_s^2)M_1^2 - M_2^4(2M_1^2 + M_2^2)m_c^3m_s^3\big]\big\} \\
&\times \langle\bar{s}s\rangle \ , \qquad \text{(A16)} \\
\hat{B}f_5^{(5)} &= \frac{{\rm e}^{-m_c^2/M_1^2 - m_s^2/M_2^2}}{24M_1^8M_2^8} \\
&\times \big\{M_2^4(M_1^2 + M_2^2)m_sm_c^5 \\
&- M_2^2(M_1^2 + M_2^2)\big[3M_1^2M_2^2 - (M_1^2 + 2M_2^2)m_s^2\big]m_c^4 \\
&+ M_2^2m_s\big[(3M_1^4 + 4M_2^2M_1^2 + M_2^4)m_s^2 \\
&- 2M_1^2M_2^2(5M_1^2 + 3M_2^2)\big]m_c^3 \\
&+ \big[2M_1^4(M_1^2 + 3M_2^2)M_2^4 \\
&+ (M_1^6 + 4M_2^2M_1^4 + 3M_2^4M_1^2)m_s^4 \\
&- 2(3M_2^2M_1^6 + 5M_2^4M_1^4)m_s^2\big]m_c^2 \\
&+ M_1^2m_s\big[4M_1^2(M_1^2 + 3M_2^2)M_2^4 \\
&+ 2(M_1^4 + 3M_2^2M_1^2 + M_2^4)m_s^4 \\
&+ (M_2^6 - 8M_1^2M_2^4 - 13M_1^4M_2^2)m_s^2\big]m_c \\
&+ M_1^4\big[4M_1^2M_2^6 + (M_1^2 + M_2^2)m_s^2(2M_2^4 + m_s^4) \\
&- (M_2^4 + 5M_1^2M_2^2)m_s^4\big] \\
&+ q^4\big[M_2^2(m_s^2 - 3M_2^2)M_1^4 + M_2^4m_cm_sM_1^2\big] \\
&- q^2\big[(2(M_1^2 + 3M_2^2)M_2^4 + (M_1^2 + 2M_2^2)m_s^4 \\
&- 2(2M_2^4 + 3M_1^2M_2^2)m_s^2)M_1^4 \\
&+ M_2^2m_cm_s(M_2^4 - 10M_1^2M_2^2 + (3M_1^2 + 2M_2^2)m_s^2)M_1^2 \\
&+ M_2^2m_c^2\big((2M_1^2 + 3M_2^2)m_s^2 - 3(M_2^4 + 2M_1^2M_2^2)\big)M_1^2 \\
&+ M_2^4(2M_1^2 + M_2^2)m_c^3m_s\big]\big\} \times g\langle\bar{s}\sigma TGs\rangle \ . \qquad \text{(A18)}
\end{aligned}$$

References

1. M.A. Shifman, A.I. Vainshtein, V.I. Zakharov, Nucl. Phys. B **147**, 385–448 (1979)
2. T.M. Aliev, V.L. Eletskii, Ya.I. Kogan, Sov. J. Nucl. Phys. **40**, 527 (1984)
3. A.A. Ovchinnikov, V.A. Slobodenyyuk, Z. Phys. C **44**, 433 (1989); V.N. Baier, Grozin, Z. Phys. C **47**, 669 (1990)
4. A.A. Ovchinnikov, Sov. J. Nucl. Phys. **50**, 519 (1989)
5. P. Ball, V.M. Braun, H.G. Dosch, Phys. Rev. D **44**, 3567 (1991)
6. P. Ball, Phys. Rev. D **48**, 3190 (1993)
7. P. Colangelo, F. De Fazio, Phys. Lett. B **520**, 78 (2001)
8. K. Kodama et al. (FNAL E653 Collab.), Phys. Lett. B **309**, 483 (1993)
9. P.L. Frabetti et al. (FNAL E687 Collab.), Phys. Lett. B **328**, 187 (1994)
10. P. Avery et al. (CLEO Collab.) Phys. Lett. B **337**, 405 (1994)
11. E.M. Aitala et al. (FNAL E791 Collab.), Phys. Lett. B **450**, 294 (1999)
12. I. Bediaga, M. Nielsen, hep-ph/0304193
13. L.J. Reinders, H. Rubinstein, S. Yazahi, Phys. Rep. **127**, 1 (1985)
14. R.E. Cutkosky, J. Math. Phys. **1**, 429 (1960)
15. B.L. Ioffe, A.V. Smilga, Nucl. Phys. B **216**, 373 (1983)
16. V.A. Fock, Phys. Z. SU **12**, 404 (1937); J. Schwinger, Particles, Sources and Fields (Addison-Wesley 1973); M.A. Shifman, Nucl. Phys. B **173**, 13 (1980); M.S. Dubovikov, A.V. Smilga, Nucl. Phys. B **185**, 109 (1981)
17. A.V. Smilga, Yad. Fiz. **35**, 473 (1982) [Sov. J. Nucl. Phys. **35**, 271 (1982)]
18. M.A. Shifman, Nucl. Phys. B **173**, 13 (1980)
19. L.D. Landau, Nucl. Phys. **13**, 181 (1959)
20. S. Narison, QCD spectral sum rules (World Scientific, Singapore 1989)
21. For a recent review article, see P. Colangelo, A. Khodjamirian, in "At the Frontier of Particle Physics / Handbook of QCD", edited by M. Shifman, World Scientific, Singapore (2001), hep-ph/0010175
22. Particle Data Group, K. Hagiwara et al., Phys. Rev. D **66**, 010001 (2002)